

IEEE P802.15
Wireless Personal Area Networks

Project	IEEE P802.15 Working Group for Wireless Personal Area Networks (WPANs)		
Title	UWB Channel Model for under 1 GHz		
Date Submitted	[12 September 2004] [rev3: 01 Nov 2004]		
Source	[Kai Siwiak] [TimeDerivative] [Coral Springs, FL]	Voice: Fax: E-mail:	[+1 954-937-3288] [] [k.siwia@ieee.org]
Re:	Adjunct to TG4a channel model document.		
Abstract	This paper presents a channel model for UWB pulse systems operating at frequencies below 1 GHz.		
Purpose	The purpose of this document is to provide IEEE P802.15 with a 100 MHz-1 GHz channel model for evaluating location aware wireless systems.		
Notice	This document has been prepared to assist the IEEE P802.15. It is offered as a basis for discussion and is not binding on the contributing individual(s) or organization(s). The material in this document is subject to change in form and content after further study. The contributor(s) reserve(s) the right to add, amend or withdraw material contained herein.		
Release	The contributor acknowledges and accepts that this contribution becomes the property of IEEE and may be made publicly available by P802.15.		

Revision History

Preliminary Draft	10 Sep 2004.
r0	12 Oct 2004.
r1	18 Oct 2004. Improved descriptions and detailed write-up.
r2	<p>27 Oct 2004. Modifications recommended by the TG4a channel model committee.</p> <p>(i) “For the LOS case, each of the deterministic rays is seen as the center of a cluster; each cluster having several components.” <i>The wall reflections were modified to add delayed reflection component due to transmission through, and reflection from the other side of the wall. The result is a single additional term for each primary wall reflection. Thus all energy terms up to about 30 dB below the direct component are included.</i></p> <p>(ii) “The amplitude distribution of the fading of the clusters has to be specified.” <i>The added fading clusters are deterministic. They are based on an additional reflection from the back side of a wall. An additional wall thickness parameter with an initial value of 12 cm has been added.</i></p> <p>(iii) “Measurement results, especially the model of Cassioli et al., should be used as much as possible to parameterize the model. Room dimensions should be chosen such that the resulting impulse responses agree reasonably well with those measurement results.” <i>The room parameters are a model input. The dimensions chosen match the delay characteristics in Cassioli et al., for the distances involved.</i></p> <p>(iv) “Pathloss exponent and attenuation at 1m distance needs to be included.” <i>The path loss exponent is already a part of the model since the preliminary draft. Spherical wave propagation is assumed for all paths (path loss exponent is thus 2) as seen in Equation (24). Path amplitudes are deterministically attenuated additionally by wall reflections and transmissions.</i></p> <p>(v) “The delay spread should be independent of the distance.” <i>The distance dependency of delay spread is critical to the overall attenuation of components in NLOS conditions and is seen in [Cassioli 2002], [Yano 2002] and [IEEE802 02/282]. It is relevant to how energy can be gathered by a receiver employing rake or channel equalization. Representative distances can be selected as desired.</i></p>
r3	Modified Equations (24), (25), (26) and (36).

15-04-0505-00-004a-UWB Channel Model for under 1 GHz

Introduction

The 100 MHz to 1,000 MHz channel model was designed with simplicity in mind, and with a direct physical interpretation for impulses and impulse doublets. There is no channel model in the current literature that applies to impulse doublets which spread energy over a 200% bandwidth. This model comprises two components.

The **first model case** is a *deterministic* line of sight (LOS) in-room model that captures the major reflection sources at low frequencies. These reflections are the room walls and floor for the LOS case. All components to about 30 dB below the direct component are captured. The ceiling is omitted. A total of 14 deterministic paths are included. Deterministic models are not unprecedented [Canada 2004]; they can provide a mechanism for studying impulse and pulse distortions.

The **second model case** is a non-line of sight (N-LOS) model which is based on the Jakes [Jakes 1974] model with exponential energy density profile (EDP) and with the addition of directly radiated energy, thus the statistics can be described by a Ricean distribution. The multipath UWB pulses and impulses are exponentially distributed, their arrival interval is randomly distributed in windows of duration T_s . The delay spread increases with distance, as is observed in experiment, thus a physically realistic propagation law naturally evolves from the model.

For both the LOS and NLOS cases a signal $S(t)$ contains all of the multipath components, weighted by the receiver antenna aperture A_e , and by the receiver antenna efficiency η_{ant} . The formulation of the multipath components, along with the time definition of UWB impulses, and the frequency dependent receiver antenna aperture and efficiency uniquely address the needs of a 100 – 1,000 MHz channel model. The method of signal detection, including the receiver filter and multiplication by the receiver template, and the signal processing will determine which and how many and how efficiently the multipath components are utilized, and how accurately ranges are determined.

The model is capable of evaluating UWB impulse radios in:

- (1) direct free space propagation considering additive white Gaussian noise (AWGN),
- (2) LOS conditions with multipath typical of a room, and
- (3) a range on N-LOS conditions with and without direct path contributions.

The model output is a signal profile in time which is the input to the UWB receiver. The full model code, rendered in Mathcad, is given in the Appendix.

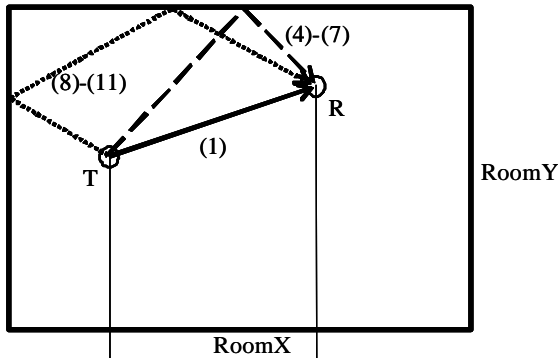
Case 1: The Line of Sight Model

LOS attenuation is free space integral over PSD for distances: $d < (RoomX^2 + RoomY^2)^{1/2}$ m
 Where *RoomX* and *RoomY* are the room dimensions. Multipath is derived from a direct path and 13 primary reflections of a room model:

- 4 principal reflections from the walls (of order $\Gamma_m = -5$ dB)
- 1 ground reflection (of order $\cos(\theta)\Gamma_m = -7$ dB)
- 4 principal corner reflections (of order $\Gamma_m^2 = -10$ dB)
- 4 secondary reflections from the walls (of order $(1+\Gamma_m)^2\Gamma_m = -21$ dB)

The amplitude order estimates above do not include the additional path attenuation which is taken into account in the model. The next order reflection would include double internal wall bounces (-35 dB), and internal wall reflections involving a corner (-29+ dB). Thus, including path incremental increases, components up to 30 dB lower than the direct component are taken into account. Multiple realizations are utilized by randomly selecting a transmit and a receive point in the room. The selected points are no closer than d_i from any wall.

Top view



Side view

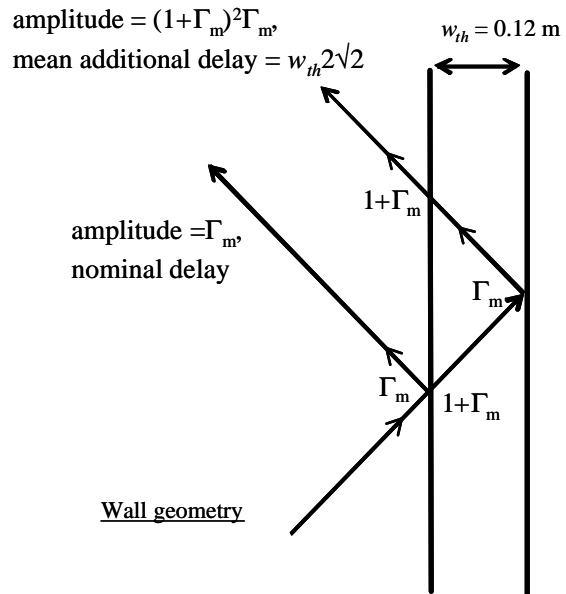
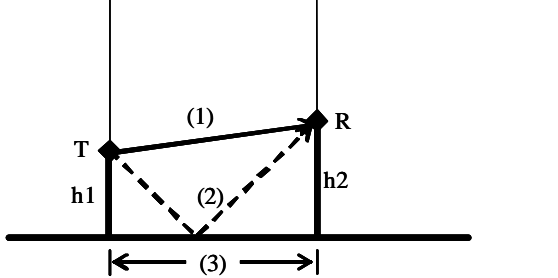


Figure 1. LOS components in a room of dimensions *RoomX* by *RoomY*. The wall secondary reflections are pictured on the right.

The LOS case of the channel model comprises 5 geometrical parameter and 3 signal parameters:

- Room dimensions *RoomX* and *RoomY*,

- Minimum distance to a wall dt ,
- Wall thickness w_{th}
- Antenna heights h_1 and h_2
- Average wall and floor reflection coefficient Γ_m
- Radiated power spectral density $EIRP_{sd}(f)$
- Receiver antenna aperture A_e and antenna efficiency $\eta_{ant}(f)$

The reflection coefficient is derived from [Honch 1992]. Figure 1 shows the signal paths between a transmit antenna T and a receive antenna R in an LOS condition in the room. Total energy is accounted for in the room. The "excess" energy in the room should be balanced by the average wall-transmitted energy. The signal paths are:

- Direct path given by Equation (1),
- Ground (floor) reflection given by (2),
- Single wall reflections given by (4) through (7),
- Double wall reflections (corner bounces) given by (8) through (11)
- The effect of internal wall reflections is captured in Equations (16) through (18).

Secondary reflections which capture the main internal wall reflected energy, shown on the right side of Figure 1, are included. The derived parameters include:

- Multipath signal profile $S(t)$
- RMS delay spread τ_{rms} ,
- the mean ray arrival rate T_s
- excess energy factor in the room is W_x

The apparent total energy received at R is greater than would be obtained from a single path free space transmission from T because the reflections direct additional time dispersed signal copies to the receiver. It is important to note that the wave propagation along each path is governed by the physics of an expanding spherical wave, thus the energy in each path attenuates as the square of distance. The case resembles a Ricean distribution comprising significant energy in a direct path followed by a decaying multipath profile. On the average, in a 3.7 m by 4.6 m room, the energy in the multipath components is 2.2 dB below the direct path energy, thus the total available energy is 2 dB higher than contained in just the direct path. The statistics of the multipath components are nearly, but not quite described by a Rayleigh distribution.

Energy conservation dictates that the total energy leaving the room should equal the energy transmitted. This can be approximately checked by observing the product of the excess energy factor with the average transmission coefficient $W_x[1 - \Gamma_m^2]$ which should be approximately one. The modeled case verifies this within approximately 0.29 dB.

The LOS model is specified by Equation (26), and supported by Equations (23), (24), and (25) in the Appendix. Specifically, the direct component and the multipath components are given by

$$\begin{aligned}
H_{LOS}(t) := & Vfs_i(d) + \left[\Gamma_m \left(\frac{Dg_i}{Gr_i} \right) \cdot Vfs(d + eG) \cdot \delta \left(t - \frac{eG}{c} \right) \right] \dots \\
& + \left[\Gamma_m \left(Vfs_i(d + eR1) \cdot \delta \left(t - \frac{eR1}{c} \right) \dots \right. \right. \\
& \quad \left. \left. + Vfs_i(d + eR2) \cdot \delta \left(t - \frac{eR2}{c} \right) \dots \right. \right. \\
& \quad \left. \left. + Vfs_i(d + eR3) \cdot \delta \left(t - \frac{eR3}{c} \right) \dots \right. \right. \\
& \quad \left. \left. + Vfs_i(d + eR4) \cdot \delta \left(t - \frac{eR4}{c} \right) \right) \right] \\
& + \Gamma_m^2 \left(Vfs_i(d + eC1) \cdot \delta \left(t - \frac{eC1}{c} \right) \dots \right) \dots \\
& \quad \left(Vfs_i(d + eC2) \cdot \delta \left(t - \frac{eC2}{c} \right) \dots \right) \dots \\
& \quad \left(Vfs_i(d + eC3) \cdot \delta \left(t - \frac{eC3}{c} \right) \dots \right) \dots \\
& \quad \left(Vfs_i(d + eC4) \cdot \delta \left(t - \frac{eC4}{c} \right) \right) \dots \\
& + \Gamma_m (1 + \Gamma_m)^2 \left(Vfs_i(d + eR1 + eW) \cdot \delta \left(t - \frac{eR1}{c} - eW \right) \dots \right) \\
& \quad \left(+ Vfs_i(d + eR2 + eW) \cdot \delta \left(t - \frac{eR2}{c} - eW \right) \dots \right) \\
& \quad \left(+ Vfs_i(d + eR3 + eW) \cdot \delta \left(t - \frac{eR3}{c} - eW \right) \dots \right) \\
& \quad \left(+ Vfs_i(d + eR4 + eW) \cdot \delta \left(t - \frac{eR4}{c} - eW \right) \right) \dots
\end{aligned} \tag{23}$$

Although many details would need to be worked out, a set of statistical components could be appended to the first order wall reflection. The component amplitude is given in terms of distance

$$Vfs(d) := \sqrt{\frac{\mu \cdot c}{4\pi}} \cdot \frac{1}{d} \tag{24}$$

The received energy is given in terms of a constant directivity antenna with efficiency $\eta_{ant}(f)$ and weighted by the emitted energy density profile EIRPsd(f)

$$W_{rx} := \frac{1.5}{4\pi} \cdot \frac{1}{f_2 - f_1} \cdot \left[\int_{f_1}^{f_2} \left(\frac{c}{f} \right)^2 \cdot \eta_{ant}(f) \cdot EIRPsd(f) df \right] \tag{25}$$

Notice that Equation (25) explicitly takes into account the emitted field strength weighting of the receiver antenna aperture area, and that the receiver antenna efficiency is specifically taken into account. Finally, the received signal is

$$S(t) := H_{LOS}(t) \cdot \sqrt{W_{rx}} \tag{26}$$

The Mathcad code for the LOS model contains a rich set of test cases and illustrative plots showing the behavior of the various components. For example:

Figure 2 shows a random sampling of transmitter (red) and receiver (blue) locations within a room of dimensions *RoomX* and *RoomY*.

Figure 3 shows the images in the walls of the points shown in Figure 2. These image points are used to calculate the various reflection distances and differential delays.

Figure 4 shows the calculated energy profiles vs. differential delay for wall reflections involving the *RoomY* dimension of the room.

Figure 5 shows the calculated energy profiles vs. differential delay for wall reflections involving the *RoomX* dimension of the room. Since the room is not square, this EDP differs visibly from the one in Figure 4.

Figure 6 shows the EDP for the ground reflection. This energy component is closely related to the direct path energy, hence the profile has definite structure.

Figure 7 shows the EDP for the four corner reflections within the room.

Figure 8 is a depiction of the room and floor reflection coefficient.

Figures 9 and 10 compare an EDP sampling of wall and corner reflected energy and compares the points with an exponentially distributed profile having the same RMS delay spread.

Figure 11 shows EDPs for the four major paths: the black points are primary wall reflections, the red points correspond to corner reflections, the blue points are ground reflections, and the green points are wall reflection involving one internal wall bounce.

Figure 12 and 13 show one particular case of multipath: Figure 12 shows the reflection amplitudes, while Figure 13 shows the energies.

Figure 14 shows a composite of a large number of LOS channel model impulse realizations. The red impulses are single wall reflections, hence the negative amplitudes. The green impulses are corner reflections which involve two reflections, hence the positive amplitudes. The black impulses represent ground reflected energy, and the magenta impulses are wall reflections that include two reflections internal to the wall.

Figures 11 and 14 show the same impulse responses plotted on two different presentations. In each case it is apparent that there is a definite relationship among the four impulse components, as can be expected from a deterministic model. The behavior of the impulse responses is

generally as noted in the measurements of Ghassemzadeh et al., in [IEEE802 04/504]. That is, the first component is strongest followed by a nearly exponential decrease in the impulse components.

Case-2: The Non-Line of Sight Multipath Model:

The non line of sight path is described by a modified Ricean EDP. This allows for parametric studies involving a direct component along with a diffuse component. Ranging errors can thus be studied with the fraction of direct path energy as a parameter. As such a total of 3 Ricean parameters plus an additional distance parameter totally specify the multipath profile. The multipath increases with distance, see [Siwiak 2003], [Cassioli 2002], and Ghassemzadeh et al., in [IEEE802 02/282]. Here it is modeled by square root of distance d/D_t scaled by the constant τ_0 . Energy dispersed into and increasingly longer multipath profile naturally results in an increase in the power law of propagation attenuation. Thus the increase by the square root of distance results in an overall inverse 2.5 power of distance for multipath components. Rather than a non-physical “phase parameter”, a random distance variation within the mean interval T_m is used to define the time that multipath components arrive at the receiver. Total energy propagates as an expanding spherical wave, so the basic propagation is inverse square law, just like the LOS case. The unit energy is allocated a fraction K_F for the direct component, if any, and $(1-K_F)$ for the multipath energy.

The following parameters specific the UWB radio performance in a N-LOS condition:

- RMS delay spread parameter τ_0 s, and initial distance D_t
- Mean interval between rays T_m s
- Fraction of energy in direct component K_F
- Radiated power spectral density EIRPsd(f)
- Receiver antenna aperture A_e and antenna efficiency $\eta_{\text{ant}}(f)$

The channel model signal profile is

- Multipath signal amplitude profile $S_N(t)$

Figure 15 illustrates multiple realizations of the diffuse component of the channel impulse response for a case at a fixed distance. An exponential delay envelope is superimposed for comparison.

The recommended parameters are $\tau_0=5.5$ ns, and $D_t=1$ m to approximately match the NLOS parameters of CM2, CM3, and CM4 in [IEEE802 02/249] at the required distances, see slide 34 of [IEEE802 04/504]. Specific recommended distances are 5, 10, 20 and 30 m. Direct path energy fraction K_F is a parameter that takes on values between 0 for a fully diffuse multipath and 1 for a pure line of sight free space path. K_F is related to the usual Ricean K -factor by $K_F=K/(1+K)$ or equivalently $K=K_F/(1-K_F)$, where K_F is in the range $[0, 1]$ and correspondingly K_F takes on the range $[0, \infty]$. Recommended values of K_F are 0 (a fully diffused multipath, 0.3 (half the reflected

energy fraction in the LOS case), and 0.6. $K_F=1$ should be used to establish the radio performance in AWGN.

For both channel model components, the signal $S_N(t)$ contains all of the multipath components, weighted by the receiver antenna aperture, and by the receiver antenna efficiency. The method of signal detection, signal convolution the receiver filter, multiplication by the receiver template, and the signal processing will determine which and how many and how efficiently the multipath components are utilized.

The N-LOS model is entirely specified by Equation (36), and supported by Equations (24), (25) given earlier, along with (35) and (37), as seen in the Appendix. The multipath field is given by

$$H_{NLOS}(t) := Vfs(d) \cdot \sqrt{Kf} \cdot \delta(0) + \left(\sqrt{1 - Kf} \cdot \sum_{k=0}^{Kmax} h_k \cdot \delta(t - Ts_k) \right) \left(Vfs(d + c \cdot Ts_k) \delta\left(t - \frac{Ts_k}{c}\right) \right) \quad (35)$$

and the received signal is

$$S_N(t) := H_{NLOS}(t) \cdot \sqrt{Wrx} \quad (36)$$

The delay spread profile is defined by

$$\tau_{rmsN}(d, Dt, \tau) := \tau_0 \cdot \sqrt{\frac{d}{Dt}} \quad (37)$$

Recommended specific values for d are 5, 10, 20 and 30 m resulting in the corresponding RMS delay spread values of approximately 12, 17, 25 and 30 ns.

References

- [Cassioli 2002] D. Cassioli, Moe Z. Win and Andreas F. Molisch, "The Ultra-Wide Bandwidth Indoor Channel: from Statistical Model to Simulations", IEEE Journal on Selected Areas on Communications, Vol. 20, pp. 1247-1257, August 2002.
- [Canada 2004] Canada, INFORMATION DOCUMENT, "Characterization of ultra-

wideband (UWB) pulse distortion in time domain,” ITU Document 1-8/203-E, 27 October 2004.

- [Honch 1992] W. Honcharenko, H. L. Bertoni, "Mechanisms governing UHF propagation on single floors in modern office buildings," IEEE Transactions on Vehicular Technology, Vol. 41, No. 4, November 1992, pp. 496-504.
- [IEEE802 02/249] “Channel Modeling Sub-committee Report – Final,” IEEE P802.15 Working Group for Wireless Personal Area Networks (WPANs), IEEE document P802.15-02/249r0-SG3a, Dec, 2002. (Online): <http://grouper.ieee.org/groups/802/15/pub/2002/Nov02/>
- [IEEE802 02/282] “UWB Indoor Model,” IEEE P802.15 Working Group for Wireless Personal Area Networks (WPANs), IEEE document P802.15-02/282r1-SG3a, July 8, 2002. (Online): <http://grouper.ieee.org/groups/802/15/pub/2002/Jul02/>
- [IEEE802 04/504] IEEE P802.15 Working Group for Wireless Personal Area Networks (WPANs), IEEE document P802.15-04/504r1-TG3a, Sept, 2004, 15-04-0504-01-003a-ds-uwband-no-response-eq-sop.ppt
- [Jakes 1974] W. C. Jakes. Microwave Mobile Communications, American Telephone and Telegraph Co., 1974, reprinted: IEEE Press, Piscataway, NJ, 1993.
- [Siwiak 2003] K. Siwiak, H. L. Bertoni, and S. Yano, “On the relation between multipath and wave propagation attenuation,” Electronic Letters, 9th January 2003, Volume 39 Number 1, pp. 142-143.
- [Yano 2002] S. M. Yano: “*Investigating the ultra-wideband Indoor wireless channel*,” Proc. IEEE VTC2002 Spring Conf., May 7-9, 2002, Birmingham, AL, Vol. 3, pp. 1200-1204.

APPENDIX

Mathcad code for the 100 – 1,000 MHz Channel model Components

Although the Mathcad code contains a rich set of illustrative examples, details and check cases, the entire **case 1: LOS model** is specified by Equation (26), and supported by Equations (23), (24), and (25). Likewise, the entire **case 2: N-LOS model** is specified by Equation (36), and supported by Equations (24), (25), (35) and (37).

UWB Channel Model Components for use below 1 GHz - Kai Siwiak

Preliminary Draft: 10 Sep 2004; rev0 12 Oct 2004; rev1 18 Oct 2004; rev2 27 Oct 2004
rev3 01 Nov 2004

The 100 MHz channel model comprises two components. The first is a LOS in-room component that captures the major reflection sources at low frequencies, which are the walls and floor for the LOS case. The second is a N-LOS component which is based on the Jakes [Jakes 1974] model with exponential energy density profile (EDP). The multipath UWB pulses and impulses are exponentially distributed, their arrival interval is randomly distributed in windows of duration T_s .

For both cases a signal $S(t)$ contains all of the multipath components, weighted by the receiver antenna aperture, and by the receiver antenna efficiency. The method of signal detection, signal convolution the receiver filter, multiplication by the receiver template, and the signal processing will determine which and how many and how efficiently the multipath components are utilized.

Case 1 - The LOS Model

LOS: attenuation is free space intergal over PSD: $d < (\text{RoomX}^2 + \text{RoomY}^2)^{1/2}$ m

- Direct plus with Γ^2 power additional single reflection multipaths; Γ^4 from corner reflections
- Multipath is derived from 13 primary reflections of a room model:
 - 4 principal reflections from the walls
 - 1 ground reflection
 - 4 principal corner reflections
 - 4 secondary wall reflections
- Multiple realizations are utilized.

The following parameters specific the UWB radio performance in a room-LOS condition:

- (1) Room dimensions RoomX and RoomY, and minimum distance to a wall d_t , wall thickness w_t
- (2) Antenna heights h_1 and h_2
- (2) Radiated power spectral density EIRPsd(f)
- (3) Receiver antenna aperture A_e
- (4) Multipath signal profile $S(t)$
- (5) Average reflection coefficient Γ_m

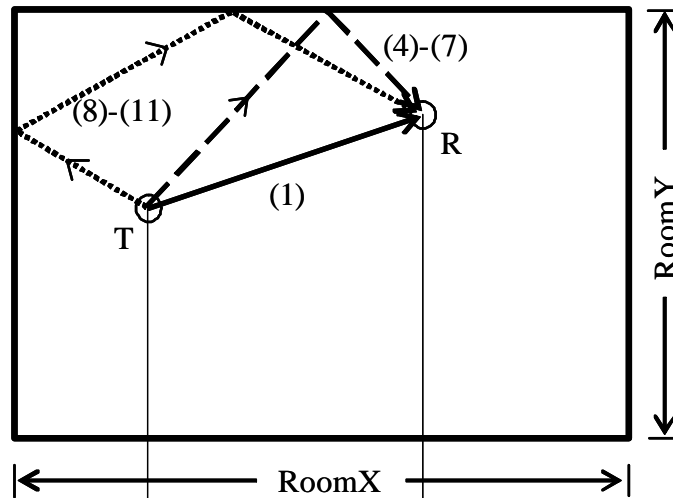
Derived parameters include:

- RMS delay spread τ_{rms} ,
- the mean ray arrival rate T_s
- excess energy factor in the room is W_x

Total energy is accounted for in the room. The "excess" energy in the room should be balanced by the average wall-transmitted energy.

The geometry for the LOS in-room model is shown in Figure 1a.

Top view



Side view

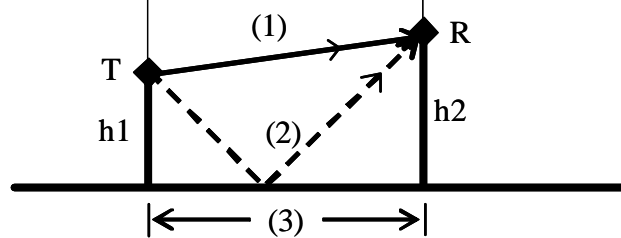


Figure 1a. Top and side views of signal paths inside a room.

Reflections are shown for only one wall and for one corner. All four wall and corners are considered in the model.

The secondary reflections from energy bouncing between walls is shown in Figure 1b.

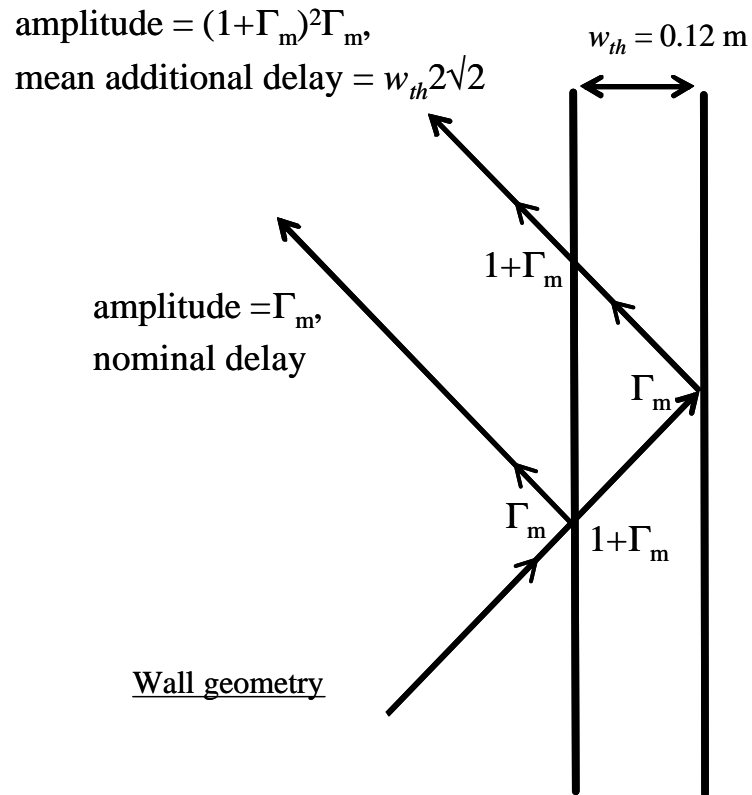


Figure 1b. Secondary reflection from the wall are attenuated about 20 dB.

Case 2 - Non-Line of Sight Multipath Model

The Jakes [Jakes 1974] model with exponential EDP will be applied, here for UWB pulses in non-line of sight (NLOS) cases. Thus the multipath impulses are exponentially distributed, their arrival interval is randomly distributed in windows of duration T_s . The delay spread parameter is a function of distance, [Siwiak 2003], and here is modeled by the square root of distance, see slide 34 of [IEEE802 04/504]. This naturally results in a 2.5 power law in propagation as a function of distance.

The following parameters specific the UWB radio performance in a N-LOS condition:

- (1) RMS delay spread parameter τ_0 s and distance D t
- (2) Mean interval between rays T_m s
- (3) Fraction of energy in direct ray K_f
- (4) Radiated power spectral density $EIRP_{sd}(f)$
- (5) Receiver antenna aperture A_e
- (6) Multipath signal profile $SN(t)$

For both channel model components, the signal $SN(t)$ contains all of the multipath components, weighted by the receiver antenna aperture, and by the receiver antenna efficiency. The method of signal detection, signal convolution the receiver filter, multiplication by the receiver template, and the signal processing will determine which and how many and how efficiently the multipath components are utilized.

References:

[Honch 1992] W. Honcharenko, H. L. Bertoni, "Mechanisms governing UHF propagation on single floors in modern office buildings," IEEE Transactions on Vehicular Technology, Vol. 41, No. 4, November 1992, pp. 496-504.

[Jakes 1974] W. C. Jakes. Microwave Mobile Communications, American Telephone and Telegraph Co., 1974, reprinted: IEEE Press, Piscataway, NJ, 1993.

[Cassoli 2002] D. Cassoli, Moe Z. Win and Andreas F. Molisch, "The Ultra-Wide Bandwidth Indoor Channel: from Statistical Model to Simulations", IEEE Journal on Selected Areas on Commun., Vol. 20, pp. 1247-1257, August 2002.

[Siwiak 2003] K. Siwiak, H. Bertoni, and S. Yano, "On the relation between multipath and wave propagation attenuation," Electronic Letters, 9th January 2003, Volume 39 Number 1, pp. 142-143.

[IEEE802 02/249] "Channel Modeling Sub-committee Report – Final," IEEE P802.15 Working Group for Wireless Personal Area Networks (WPANs), IEEE document P802.15-02/249r0-SG3a, Dec, 2002. (Online): <http://grouper.ieee.org/groups/802/15/pub/2002/Nov02/>

[IEEE802 04/504] IEEE P802.15 Working Group for Wireless Personal Area Networks (WPANs), IEEE document P802.15-04/504r1-TG3a, Sept, 2004, 15-04-0504-01-003a-ds-uwbn-response-eq-sop.ppt

Case 1: Line of Sight Multipath Model

Constants: speed of propagation, m/s	$c := 299792458$	$\mu := 4\pi \cdot 10^{-7}$
	MHz := 10^6	nanosec := 10^{-9}
Room dimensions for LOS case, m	RoomX := 3.7	RoomY := 4.6
Minimum distance from walls, and the wall thickness, m	dt := 0.1	wth := 0.12
Antenna heights above the floor, m	h1 := 1.0	h2 := 2

A room in an office or industrial area is modeled as 4 walls with dimensions RoomX and RoomY (m). The radio devices are at heights h1 and h2, and are at least distance dt from any wall. The reflection coefficient Γ is a single average value derived from [Honch 1992].

A direct path and ground reflected path between two radios in the same room is first selected randomly. Then the four principle wall reflections are considered.

The direct and ground reflected path are found from:

$$d(x1, x2, y1, y2) := \sqrt{(x2 - x1)^2 + (y2 - y1)^2 + (h2 - h1)^2} \quad (1)$$

$$gnd(x1, x2, y1, y2) := \sqrt{(x2 - x1)^2 + (y2 - y1)^2 + (h2 + h1)^2} \quad (2)$$

Separation distance projected on the ground is

$$dg(x1, x2, y1, y2) := \sqrt{(x2 - x1)^2 + (y2 - y1)^2} \quad (3)$$

The principal reflected paths are the specular images of the direct path.

$$r1(x1, x2, y1, y2) := \sqrt{(x2 - x1)^2 + (y2 + y1)^2 + (h2 - h1)^2} \quad (4)$$

$$r2(x1, x2, y1, y2) := \sqrt{(x2 - x1)^2 + (2 \cdot \text{RoomY} - y2 - y1)^2 + (h2 - h1)^2} \quad (5)$$

$$r3(x1, x2, y1, y2) := \sqrt{(x2 + x1)^2 + (y2 - y1)^2 + (h2 - h1)^2} \quad (6)$$

$$r4(x1, x2, y1, y2) := \sqrt{(2 \cdot \text{RoomX} - x2 - x1)^2 + (y2 - y1)^2 + (h2 - h1)^2} \quad (7)$$

Corner bank reflection paths - two wall reflections - there are two possibilities for projecting each corner image, but both result in the same path distance:

$$c1(x1, x2, y1, y2) := \sqrt{(x2 + x1)^2 + (y2 + y1)^2 + (h2 - h1)^2} \quad (8)$$

$$c2(x1, x2, y1, y2) := \sqrt{(x2 + x1 - 2 \cdot \text{RoomX})^2 + (y2 + y1)^2 + (h2 - h1)^2} \quad (9)$$

$$c3(x1, x2, y1, y2) := \sqrt{(x2 + x1 - 2 \cdot \text{RoomX})^2 + (y2 + y1 - 2 \cdot \text{RoomY})^2 + (h2 - h1)^2} \quad (10)$$

$$c4(x1, x2, y1, y2) := \sqrt{(x2 + x1)^2 + (y2 + y1 - 2 \cdot \text{RoomY})^2 + (h2 - h1)^2} \quad (11)$$

Equations (1)-(11) are exercised to compute a statistically significant number of randomly selected paths in the room, and the specular reflected paths are also computed. Nrnd is the counter limit for index i and is set to several thousands to get statistically valid results. Coordinates $(XR1_i, YR1_i)$ and $(XR2_i, YR2_i)$ of the two direct path endpoints are selected.

Number of trials is: Nrnd := 2000 $i := 0..Nrnd$

$$\begin{aligned} X1r_i &:= \text{rnd}(\text{RoomX} - 2 \cdot \text{dt}) + \text{dt} & Y1r_i &:= \text{rnd}(\text{RoomY} - 2 \cdot \text{dt}) + \text{dt} \\ X2r_i &:= \text{rnd}(\text{RoomX} - 2 \cdot \text{dt}) + \text{dt} & Y2r_i &:= \text{rnd}(\text{RoomY} - 2 \cdot \text{dt}) + \text{dt} \end{aligned} \quad (12)$$

Then the direct D_i distances and ground reflected Gr distances are computed, and the principle specular wall reflection distances $R1_i, R2_i, R3_i, R4_i$ are computed. Corner reflection $C1, C2, C3, C4$ are found. The path lengths in excess of the direct path are $eR1_i, eR2_i, eR3_i, eR4_i$; and $eC1, eC2, eC3, eC4$.

$$\begin{aligned} D_i &:= d(X1r_i, X2r_i, Y1r_i, Y2r_i) & Dg_i &:= dg(X1r_i, X2r_i, Y1r_i, Y2r_i) \\ R1_i &:= r1(X1r_i, X2r_i, Y1r_i, Y2r_i) & eR1_i &:= R1_i - D_i \\ R2_i &:= r2(X1r_i, X2r_i, Y1r_i, Y2r_i) & eR2_i &:= R2_i - D_i \\ R3_i &:= r3(X1r_i, X2r_i, Y1r_i, Y2r_i) & eR3_i &:= R3_i - D_i \\ R4_i &:= r4(X1r_i, X2r_i, Y1r_i, Y2r_i) & eR4_i &:= R4_i - D_i \\ Gr_i &:= \text{gnd}(X1r_i, X2r_i, Y1r_i, Y2r_i) & eG_i &:= Gr_i - D_i \\ C1_i &:= c1(X1r_i, X2r_i, Y1r_i, Y2r_i) & eC1_i &:= C1_i - D_i \\ C2_i &:= c2(X1r_i, X2r_i, Y1r_i, Y2r_i) & eC2_i &:= C2_i - D_i \\ C3_i &:= c3(X1r_i, X2r_i, Y1r_i, Y2r_i) & eC3_i &:= C3_i - D_i \\ C4_i &:= c4(X1r_i, X2r_i, Y1r_i, Y2r_i) & eC4_i &:= C4_i - D_i \end{aligned} \quad (13)$$

Additional mean delay due to the first order internal wall reflection is:

$$eW := 2\sqrt{2} \cdot \text{with} \quad eW = 0.339 \quad m \quad (13a)$$

View a subset of points: $xs := 300$ $x := 0..xs$

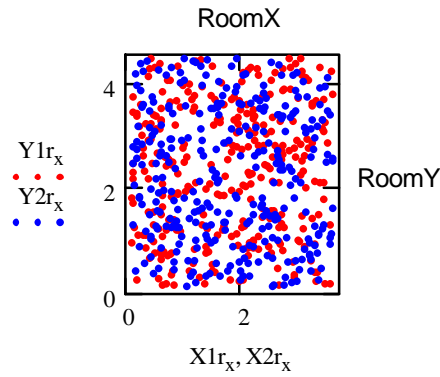


Figure 2. A sampling of the total points (X1, Y1) and (X2, Y2).

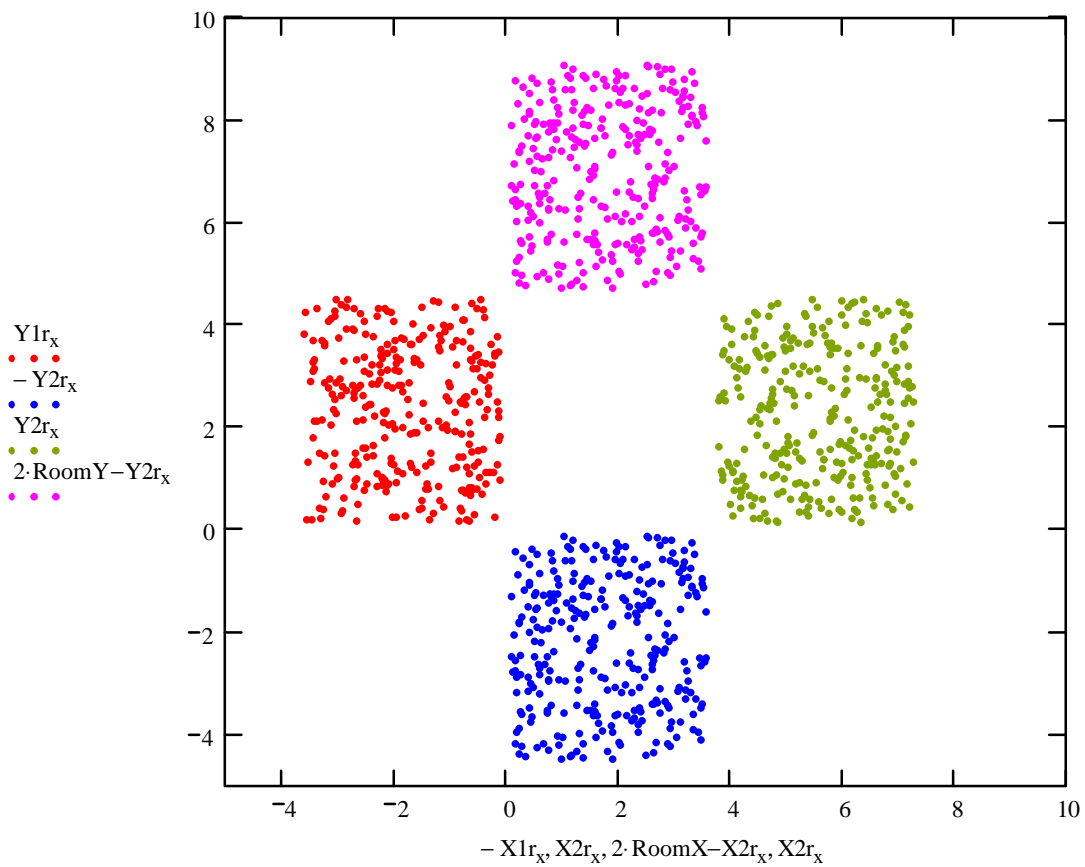


Figure 3. Images in the room walls of the reflection points. C1 are lower left and C2 are lower right, C3 are upper right and C4 are upper left.

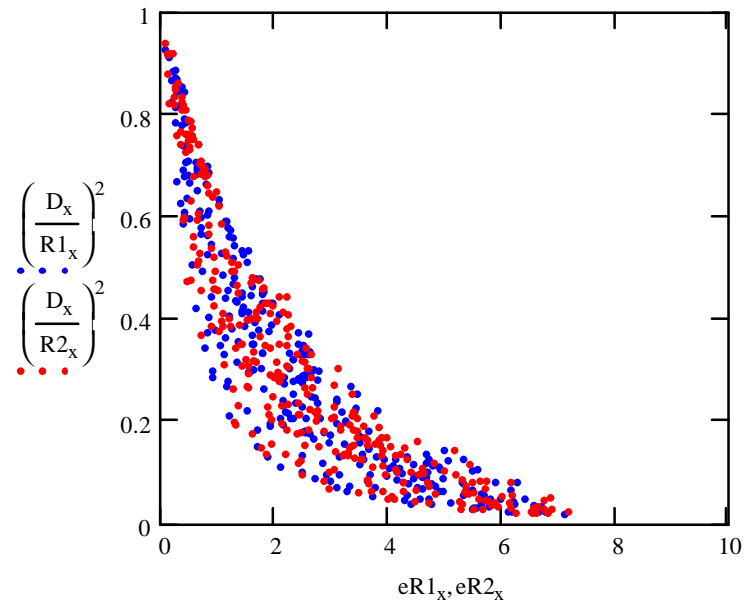


Figure 4. Energy delay profile (EDP) vs. excess delay: R1, R2. The excess delays is associated with the Y dimension of the room.

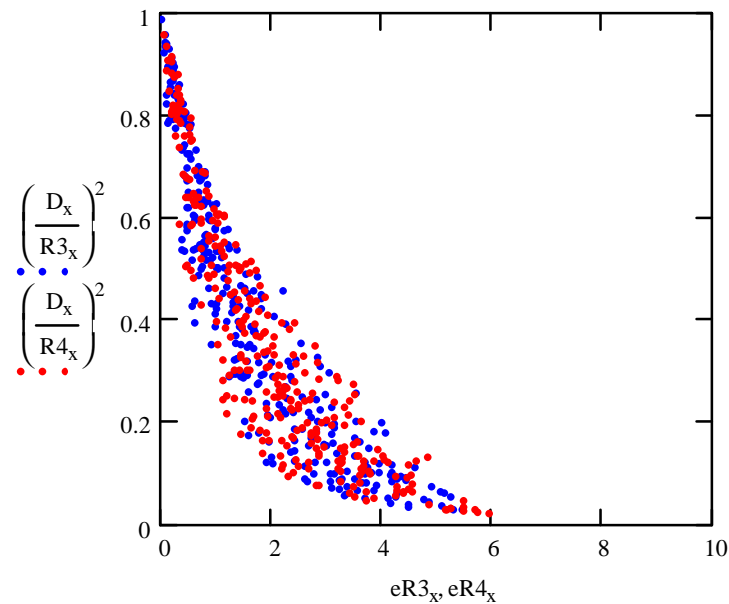


Figure 5. Energy delay profile vs. excess delay, R3, R4. The excess delays are associated with the X dimension of the room.

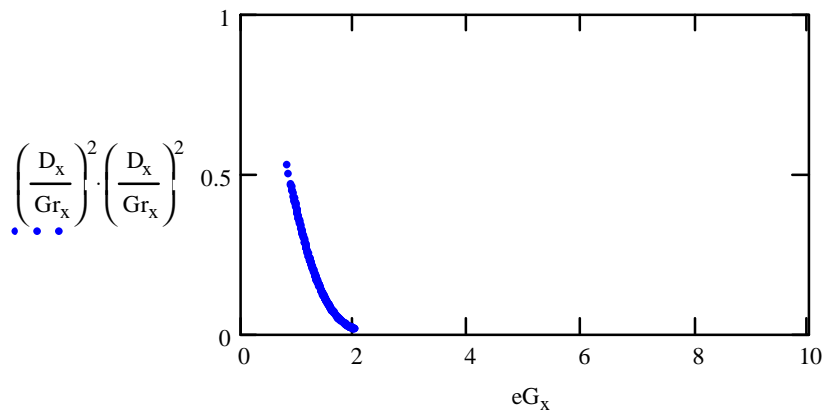


Figure 6. Energy delay profile vs. excess delay, for the ground reflection Gr .

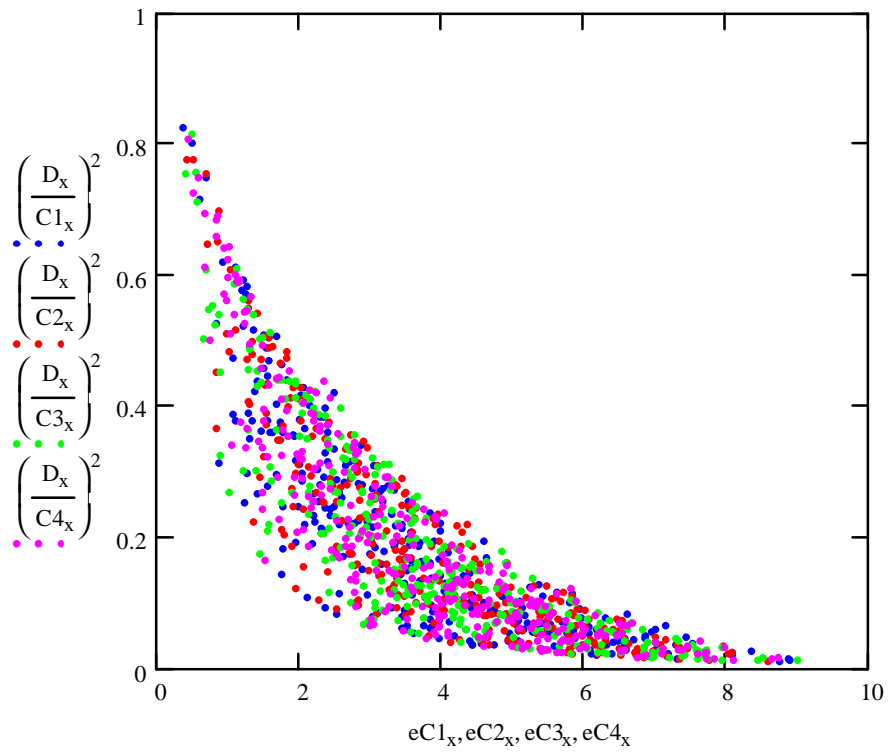


Figure 7. Energy delay profile vs. excess delay, for the corner reflections.

Reflections from the floor and walls.

Reflection coefficient from concrete or plasterboard is between 0.3 for 0 deg, 1 for grazing angle of incidence, see [Honch 1992].

$j := 0..9$

$\Gamma_j :=$	$\Gamma_j =$	$j =$
0.3	0.3	0
0.3	0.3	1
0.3	0.3	2
0.3	0.3	3
$0.3 + \frac{0.7}{5}$	0.44	4
$0.3 + 2 \cdot \frac{.7}{5}$	0.58	5
$0.3 + 3 \cdot \frac{.7}{5}$	0.72	6
$0.3 + 4 \cdot \frac{.7}{5}$	0.86	7
1	1	8
1	1	9

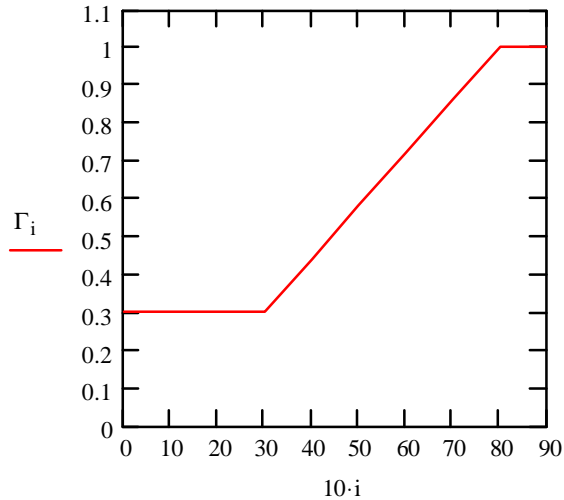


Figure 8. Reflection coefficient vs. incident angle for concrete and plaster board walls. [Honch 1992].

$$\Gamma_m := -\text{mean}(\Gamma) \quad \Gamma_m = -0.58 \quad (14)$$

$$20 \cdot \log(|\Gamma_m|) = -4.731$$

Considering transmissions through walls:

Normal incidence transmission $20 \cdot \log(1 - .3) = -3.098$

Average incidence transmission $T_m := 1 + \Gamma_m \quad 20 \cdot \log(T_m) = -7.535$

Secondary reflections involve a transmission through one wall interface followed by a reflection from the back side of the wall followed by the transmission through the front side of the wall. The secondary reflection are thus on the average down by:

$$\Gamma_{2m} := -\frac{1}{9} \cdot \sum_{j=1}^9 \left[(1 - \Gamma_j)^2 \cdot \Gamma_j + .001 \right] \quad (15)$$

$$\Gamma_{2m} = -0.085 \quad 20 \cdot \log(|\Gamma_{2m}|) = -21.428 \quad \text{dB}$$

The average secondary reflection is about 20 dB attenuated and will be included.

Higher order wall internal reflections are omitted; the next component is ~35 dB below the direct:

$$\Gamma_{3m} := -\frac{1}{9} \cdot \sum_{j=1}^9 \left[(1 - \Gamma_j)^2 \cdot (\Gamma_j)^3 + .001 \right] \quad 20 \cdot \log(|\Gamma_{3m}|) = -35.474 \quad \text{dB}$$

Second order corner reflections will be omitted, they are more than 20 dB down:

$$\Gamma_{2cm} := -\frac{1}{9} \cdot \sum_{j=1}^9 \left[(1 - \Gamma_j)^2 \cdot (\Gamma_j)^2 + .001 \right] \quad 20 \cdot \log(|\Gamma_{2cm}|) = -29.078 \quad \text{dB}$$

One secondary wall reflection is included. Its amplitude is about 20 dB below the direct component.

The additional delay of the secondary reflection is:

$$eW = 0.339 \quad \text{m}$$

The included reflection components inside the room are:

- 4 principal reflections from the walls (of order $\Gamma_m = -5$ dB)
- 1 ground reflection (of order $\cos(\theta)\Gamma_m = -7$ dB)
- 4 principal corner reflections (of order $\Gamma_m^2 = -10$ dB)
- 4 secondary reflections from the walls (of order $(1+\Gamma_m)^2\Gamma_m = -21$ dB)

Three distinct groupings of the EDP (energy delay profile) are evident in Figures 4-7. These occur because there are three distinct mechanisms in operation. The room is a rectangle so reflections associated with the width and length will cluster differently. Also the ground reflection depends only on separation distance and on antenna heights h_1 and h_2 .

The rms delay spread τ_{rms} is the second central moment of the power delay profile for each of path. The energies relative to a direct path are the square of the distance ratio: $(D/R)^2$. The ground reflected component is out of the plane of the other components, and its energy is additionally weighted by the the projection of the vertical field vector on the receive antenna, via the ground reflection hence the ground component relative energy is approximately $(1/Gr)^2(D/Gr)^4$. The delay spread is found from

$$\begin{aligned} \tau_{m_1} := & \left[\left(\frac{D_i}{R_{1_i}} \right)^2 \cdot eR_{1_i} + \left(\frac{D_i}{R_{2_i}} \right)^2 \cdot eR_{2_i} + \left(\frac{D_i}{R_{3_i}} \right)^2 \cdot eR_{3_i} + \left(\frac{D_i}{R_{4_i}} \right)^2 \cdot eR_{4_i} + \left(\frac{Dg_i}{Gr_i} \right)^2 \cdot \left(\frac{D_i}{Gr_i} \right)^4 \cdot eG_i \right] \cdot \Gamma_m^2 \dots \\ & + \left[\left(\frac{D_i}{R_{1_i}} \right)^2 \cdot (eR_{1_i} + eW) + \left(\frac{D_i}{R_{2_i}} \right)^2 \cdot (eR_{2_i} + eW) \dots \right. \\ & \quad \left. + \left(\frac{D_i}{R_{3_i}} \right)^2 \cdot (eR_{3_i} + eW) + \left(\frac{D_i}{R_{4_i}} \right)^2 \cdot (eR_{4_i} + eW) \right] \cdot \Gamma_{2m}^2 \dots \\ & + \left[\left(\frac{D_i}{C_{1_i}} \right)^2 \cdot eC_{1_i} + \left(\frac{D_i}{C_{2_i}} \right)^2 \cdot eC_{2_i} + \left(\frac{D_i}{C_{3_i}} \right)^2 \cdot eC_{3_i} + \left(\frac{D_i}{C_{4_i}} \right)^2 \cdot eC_{4_i} \right] \cdot \Gamma_m^4 \end{aligned} \quad (16)$$

$$\begin{aligned} \tau_{m_2} := & \left[\left(\frac{D_i}{R_{1_i}} \right)^2 \cdot (eR_{1_i})^2 + \left(\frac{D_i}{R_{2_i}} \right)^2 \cdot (eR_{2_i})^2 + \left(\frac{D_i}{R_{3_i}} \right)^2 \cdot (eR_{3_i})^2 \dots \right] \cdot \Gamma_m^2 \dots \\ & + \left[\left(\frac{D_i}{R_{4_i}} \right)^2 \cdot (eR_{4_i})^2 + \left(\frac{Dg_i}{Gr_i} \right)^2 \cdot \left(\frac{D_i}{Gr_i} \right)^4 \cdot (eG_i)^2 \right] \\ & + \left[\left(\frac{D_i}{R_{1_i}} \right)^2 \cdot (eR_{1_i} + eW)^2 + \left(\frac{D_i}{R_{2_i}} \right)^2 \cdot (eR_{2_i} + eW)^2 \dots \right. \\ & \quad \left. + \left(\frac{D_i}{R_{3_i}} \right)^2 \cdot (eR_{3_i} + eW)^2 + \left(\frac{D_i}{R_{4_i}} \right)^2 \cdot (eR_{4_i} + eW)^2 \right] \cdot \Gamma_{2m}^2 \dots \\ & + \left[\left(\frac{D_i}{C_{1_i}} \right)^2 \cdot (eC_{1_i})^2 + \left(\frac{D_i}{C_{2_i}} \right)^2 \cdot (eC_{2_i})^2 + \left(\frac{D_i}{C_{3_i}} \right)^2 \cdot (eC_{3_i})^2 + \left(\frac{D_i}{C_{4_i}} \right)^2 \cdot (eC_{4_i})^2 \right] \cdot \Gamma_m^4 \end{aligned} \quad (17)$$

$$W_i := \left[\left(\frac{D_i}{R1_i} \right)^2 + \left(\frac{D_i}{R2_i} \right)^2 + \left(\frac{D_i}{R3_i} \right)^2 + \left(\frac{D_i}{R4_i} \right)^2 + \left(\frac{Dg_i}{Gr_i} \right)^2 \cdot \left(\frac{D_i}{Gr_i} \right)^4 \right] \cdot (\Gamma_m^2 + \Gamma_{2m}^2) \dots$$

$$+ \left[\left(\frac{D_i}{C1_i} \right)^2 + \left(\frac{D_i}{C2_i} \right)^2 + \left(\frac{D_i}{C3_i} \right)^2 + \left(\frac{D_i}{C4_i} \right)^2 \right] \cdot \Gamma_m^4 \quad (18)$$

The "total" energy in the room is W_x times the direct path energy:

$$W_x := \text{mean}(W) + 1 \quad 10 \cdot \log(W_x) = 2.091 \quad \text{dB}$$

$$10 \cdot \log(W_x - 1) = -2.088 \quad \text{dB}$$

$$\tau_{2\text{rms}_i} := \sqrt{\frac{\text{tm}_{i,2}^2}{W_i} - \left(\frac{\text{tm}_i}{W_i} \right)^2} \quad \text{trms} := \text{mean}(\tau_{2\text{rms}}) \quad (19)$$

$$\max(\tau_{2\text{rms}}) = 1.727$$

$$\min(\tau_{2\text{rms}}) = 0.185$$

$$\text{trms} = 1.202$$

meters

Finally the rms delay spread τ_{rms} is found

$$\tau_{\text{rms}} := \frac{\text{trms}}{c} \quad (20)$$

and its value for the selected case is

$$\tau_{\text{rms}} \cdot 10^9 = 4.008 \quad \text{nS}$$

$$\frac{\max(\tau_{2\text{rms}})}{c} \cdot 10^9 = 5.761 \quad \text{nS}$$

The mean ground reflected component is

$$\text{Ground}_i := \left(\frac{D_i}{Gr_i} \right)^4 \cdot cG_i \quad \text{GdB} := \text{mean}(\text{Ground}) \quad 10 \cdot \log(\text{GdB}) = -6.792$$

Figure 9 shows the EDPs vs. excess delays for all three sets of reflections. The secondary wall reflections are not shown in this figure. Note the ground reflections (magenta) follow a narrow range of possibilities. An exponential EDP with delay spread τ_{rms} is shown as the black trace, but it does not model the room reflections very well. Since the room primary reflections are entirely deterministic, these will be used as the model. The clear areas hugging the abscissa and the ordinate result from setting the two antenna heights to different values.

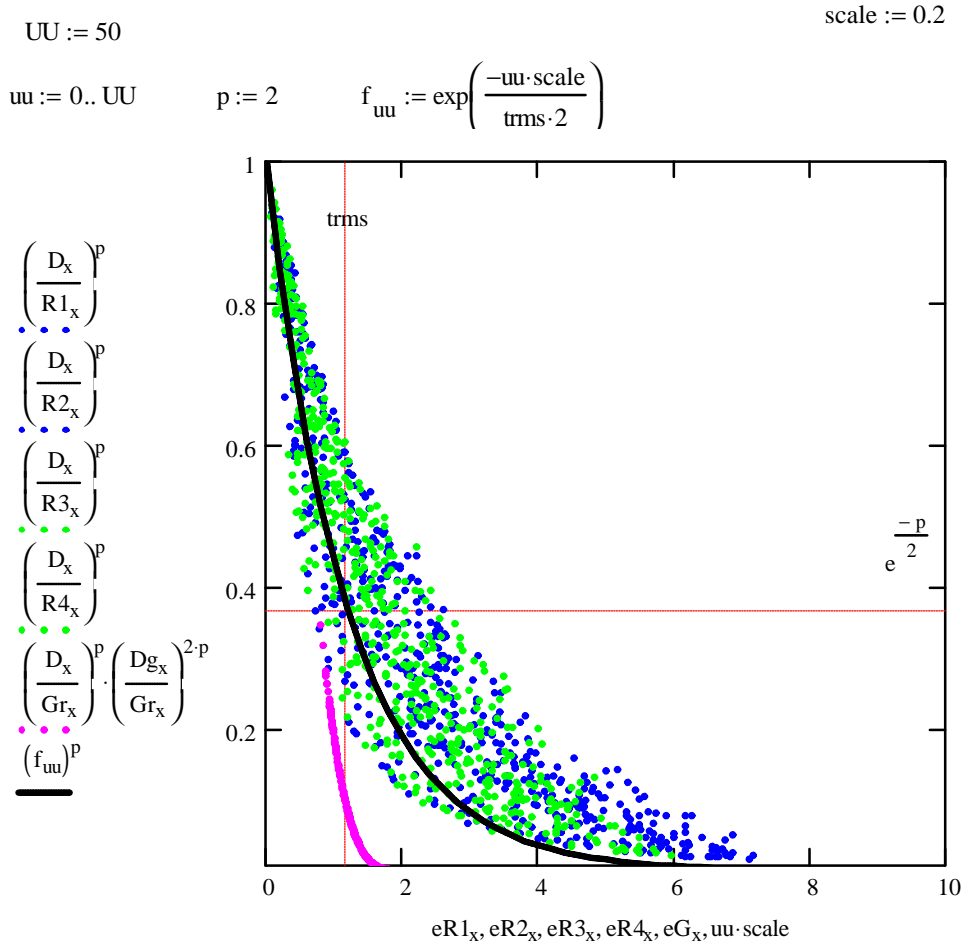


Figure 9. Energy delay profile vs. excess delay (m) for primary wall-reflected components compared with exponential EDP.

The "corner bank shots"

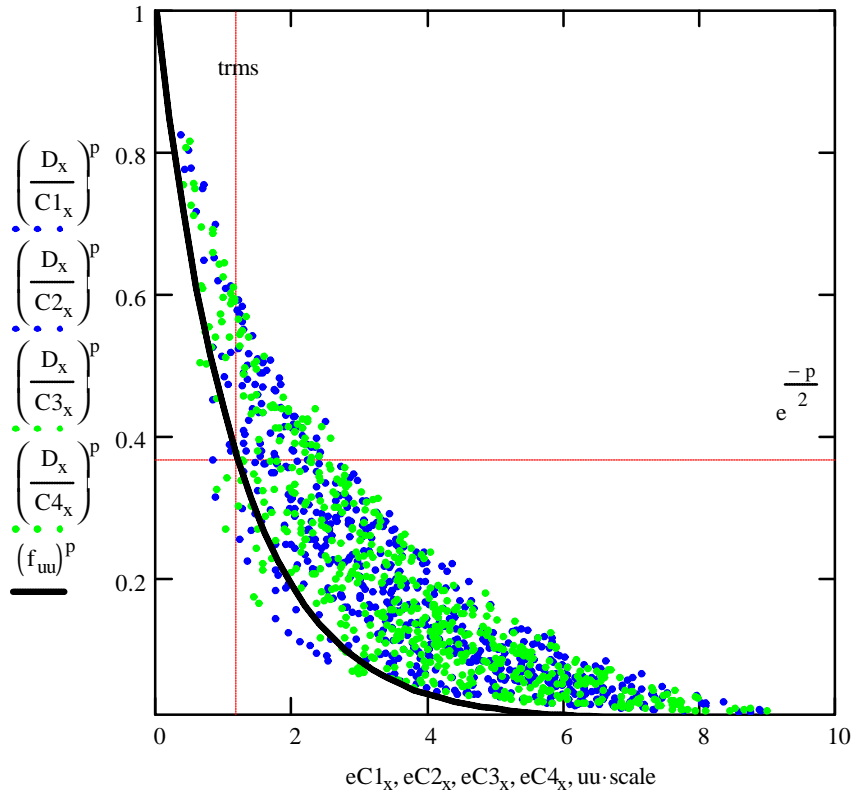


Figure 10. Energy delay profile vs. excess delay (m) for all corner reflected components compared with exponential EDP.

An exponential EDP is not a very good fit to the room calculation. Since this case is deterministic, the actual 13-reflection room model can be used.

Arrange the various components for plotting a sample:

$$p := 1$$

$$xs = 300 \quad xs4 := \text{floor}\left(\frac{xs}{4}\right) - 1 \quad xs4 = 74 \quad xx1 := 0..xs4$$

$$\text{Ref0}_{xx1} := \left(\frac{D_{xx1}}{R1_{xx1}} \cdot \Gamma_m\right)^p \quad \text{Ref1}_{xx1} := \left(\frac{D_{xx1}}{R1_{xx1}} \cdot \Gamma_{2m}\right)^p$$

$$\text{Ref0}_{xx1+1+xs4} := \left(\frac{D_{xx1}}{R2_{xx1}} \cdot \Gamma_m\right)^p \quad \text{Ref1}_{xx1+1+xs4} := \left(\frac{D_{xx1}}{R2_{xx1}} \cdot \Gamma_{2m}\right)^p$$

$$\text{Ref0}_{xx1+(1+xs4) \cdot 2} := \left(\frac{D_{xx1}}{R3_{xx1}} \cdot \Gamma_m\right)^p \quad \text{Ref1}_{xx1+(1+xs4) \cdot 2} := \left(\frac{D_{xx1}}{R3_{xx1}} \cdot \Gamma_{2m}\right)^p$$

$$\text{Ref0}_{xx1+(1+xs4) \cdot 3} := \left(\frac{D_{xx1}}{R4_{xx1}} \cdot \Gamma_m\right)^p \quad \text{Ref1}_{xx1+(1+xs4) \cdot 3} := \left(\frac{D_{xx1}}{R4_{xx1}} \cdot \Gamma_{2m}\right)^p$$

$$\text{Cor0}_{xx1} := \left(\frac{D_{xx1}}{C1_{xx1}} \cdot \Gamma_m^2\right)^p \quad \text{Cor0}_{xx1+(1+xs4) \cdot 2} := \left(\frac{D_{xx1}}{C3_{xx1}} \cdot \Gamma_m^2\right)^p$$

$$\text{Cor0}_{xx1+1+xs4} := \left(\frac{D_{xx1}}{C2_{xx1}} \cdot \Gamma_m^2\right)^p \quad \text{Cor0}_{xx1+(1+xs4) \cdot 3} := \left(\frac{D_{xx1}}{C4_{xx1}} \cdot \Gamma_m^2\right)^p$$

$$\text{Gnd}_{xx1} := \left(\frac{D_{xx1}}{Gr_{xx1}} \cdot \Gamma_m\right)^p \cdot \left(\frac{Dg_{xx1}}{Gr_{xx1}}\right)^{2 \cdot p}$$

Delays:

$$e\text{Ref1}_{xx1+(1+xs4) \cdot 0} := eR1_{xx1} + eW \quad e\text{Ref0}_{xx1+(1+xs4) \cdot 0} := eR1_{xx1} \quad e\text{Cor0}_{xx1+(1+xs4) \cdot 0} := eC1_{xx1}$$

$$e\text{Ref1}_{xx1+(1+xs4) \cdot 1} := eR2_{xx1} + eW \quad e\text{Ref0}_{xx1+(1+xs4) \cdot 1} := eR2_{xx1} \quad e\text{Cor0}_{xx1+(1+xs4) \cdot 1} := eC2_{xx1}$$

$$e\text{Ref1}_{xx1+(1+xs4) \cdot 2} := eR3_{xx1} + eW \quad e\text{Ref0}_{xx1+(1+xs4) \cdot 2} := eR3_{xx1} \quad e\text{Cor0}_{xx1+(1+xs4) \cdot 2} := eC3_{xx1}$$

$$e\text{Ref1}_{xx1+(1+xs4) \cdot 3} := eR4_{xx1} + eW \quad e\text{Ref0}_{xx1+(1+xs4) \cdot 3} := eR4_{xx1} \quad e\text{Cor0}_{xx1+(1+xs4) \cdot 3} := eC4_{xx1}$$

Energy of reflection components relative to their direct path energy. There are four distinct clusters of energy:

- (1) Wall reflected paths
- (2) Corner reflections
- (3) Wall reflections with double internal bounce
- (4) Ground reflections

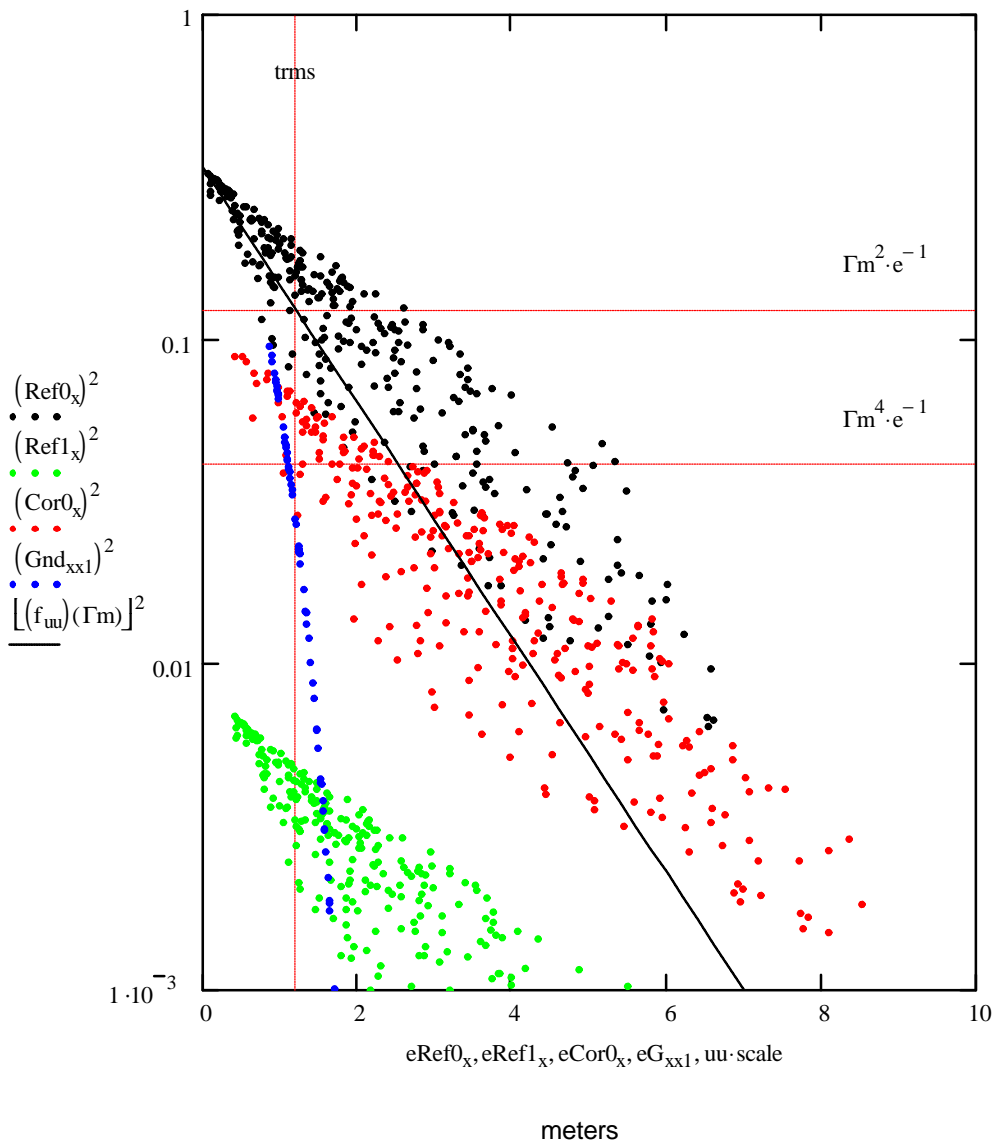


Figure 11. Multipath Energy vs. excess delay, m, for all components. Solid line represents an exponential distribution with the same delay spread.

A mean excess delay is found from

$$\text{Delay}_i := \frac{(eR1_i + eR2_i + eR3_i + eR4_i) \cdot (1 + eW) + eG_i \dots + eC1_i + eC2_i + eC3_i + eC4_i}{13} \quad (21)$$

$$D_{mn} := \text{mean}(\text{Delay}) \quad D_{mn} = 2.226 \quad \text{m}$$

$$\text{median}(\text{Delay}) = 2.259 \quad \frac{\text{median}(\text{Delay})}{c} \cdot 10^9 = 7.534 \quad \text{nanoseconds}$$

The mean ray arrival interval T_s is derived from the mean excess delay.

$$T_s := \frac{D_{mn}}{c} \quad T_s \cdot 10^9 = 7.423 \quad \text{nS} \quad (22)$$

We now have all the required components for the multipath portion of a channel model.

For the line of sight (LOS) model components, we have a direct path d , and wall reflected multipath components that carry energy in addition to the free space path between the transmitter and the receiver. The i -th realization of the in-room LOS channel impulse response field spectral density is thus:

$$H_{\text{LOS}i}(t) := Vfs_i(d) + \left[\Gamma m \left(\frac{Dg_i}{Gr_i} \right) \cdot Vfs(d + eG) \cdot \delta \left(t - \frac{eG}{c} \right) \right] \dots$$

$$+ \left[\Gamma m \cdot \left(\begin{array}{l} Vfs_i(d + eR1) \cdot \delta \left(t - \frac{eR1}{c} \right) \dots \\ + Vfs_i(d + eR2) \cdot \delta \left(t - \frac{eR2}{c} \right) \dots \\ + Vfs_i(d + eR3) \cdot \delta \left(t - \frac{eR3}{c} \right) \dots \\ + Vfs_i(d + eR4) \cdot \delta \left(t - \frac{eR4}{c} \right) \dots \end{array} \right) + \Gamma m^2 \cdot \left(\begin{array}{l} Vfs_i(d + eC1) \cdot \delta \left(t - \frac{eC1}{c} \right) \dots \\ + Vfs_i(d + eC2) \cdot \delta \left(t - \frac{eC2}{c} \right) \dots \\ + Vfs_i(d + eC3) \cdot \delta \left(t - \frac{eC3}{c} \right) \dots \\ + Vfs_i(d + eC4) \cdot \delta \left(t - \frac{eC4}{c} \right) \dots \end{array} \right) \right]$$

$$+ \Gamma m \cdot (1 + \Gamma m)^2 \cdot \left(\begin{array}{l} Vfs_i(d + eR1 + eW) \cdot \delta \left(t - \frac{eR1}{c} - eW \right) \dots \\ + Vfs_i(d + eR2 + eW) \cdot \delta \left(t - \frac{eR2}{c} - eW \right) \dots \\ + Vfs_i(d + eR3 + eW) \cdot \delta \left(t - \frac{eR3}{c} - eW \right) \dots \\ + Vfs_i(d + eR4 + eW) \cdot \delta \left(t - \frac{eR4}{c} - eW \right) \dots \end{array} \right) \quad (23)$$

and the magnetic field strength spectral density at distance d is based on a spherical wave

$$Vfs(d) := \sqrt{\frac{\mu \cdot c}{4\pi}} \cdot \frac{1}{d} \quad (24)$$

[corrected: rev 3].

$p := 1$ $m := 7$ Th m-th realization; normalized to direct component

$ua := 1..4$

Ground component:
$$G00 := \left(\frac{D_m}{Gr_m} \cdot \Gamma_m \right)^p \cdot \left(\frac{Dg_m}{Gr_m} \right)^p$$

Wall reflected components, and their delays:

$$R0_1 := \left(\frac{D_m}{R1_m} \cdot \Gamma_m \right)^p \quad R0_2 := \left(\frac{D_m}{R2_m} \cdot \Gamma_m \right)^p \quad R0_3 := \left(\frac{D_m}{R3_m} \cdot \Gamma_m \right)^p \quad R0_4 := \left(\frac{D_m}{R4_m} \cdot \Gamma_m \right)^p$$

$$eR00_1 := eR1_m \quad eR00_2 := eR2_m \quad eR00_3 := eR3_m \quad eR00_4 := eR4_m$$

Secondary wall reflections, with bounce inside the wall, and their delays:

$$R1_1 := \left(\frac{D_m}{R1_m + eW} \cdot \Gamma_{2m} \right)^p \quad R1_2 := \left(\frac{D_m}{R2_m} \cdot \Gamma_{2m} \right)^p \quad R1_3 := \left(\frac{D_m}{R3_m} \cdot \Gamma_{2m} \right)^p \quad R1_4 := \left(\frac{D_m}{R4_m} \cdot \Gamma_{2m} \right)^p$$

$$eR01_{ua} := eR00_{ua} + eW$$

Corner reflected components and their delays:

$$C0_1 := \left(\frac{D_m}{C1_m} \cdot \Gamma_m^2 \right)^p \quad C0_2 := \left(\frac{D_m}{C2_m} \cdot \Gamma_m^2 \right)^p \quad C0_3 := \left(\frac{D_m}{C3_m} \cdot \Gamma_m^2 \right)^p \quad C0_4 := \left(\frac{D_m}{C3_m} \cdot \Gamma_m^2 \right)^p$$

$$eC00_1 := eC1_m \quad eC00_2 := eC2_m \quad eC00_3 := eC3_m \quad eC00_4 := eC4_m$$

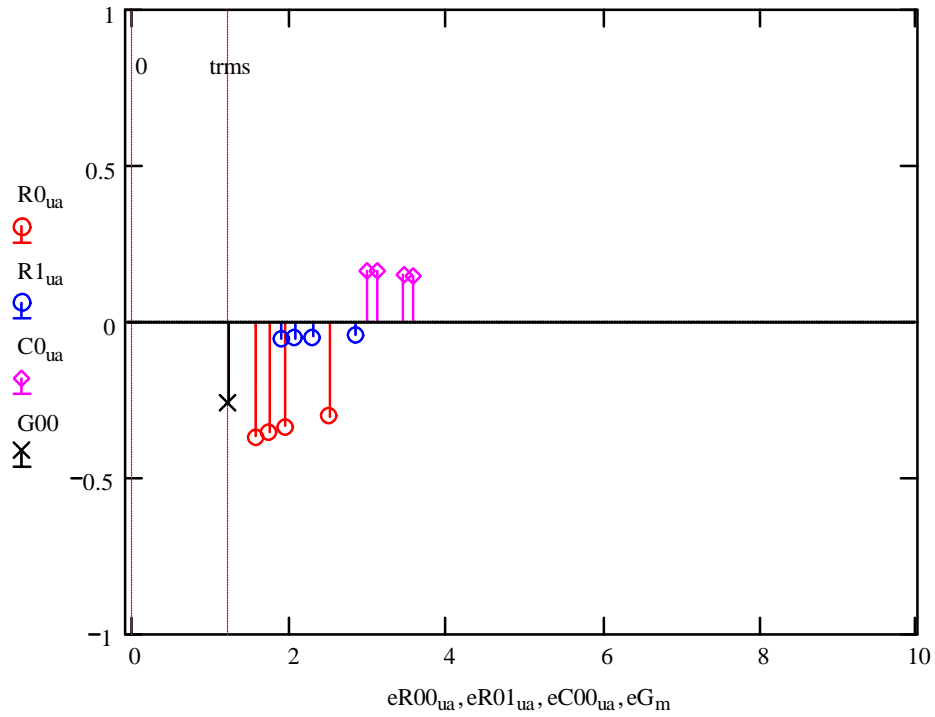


Figure 12. One particular realization of the LOS channel impulse amplitude response.

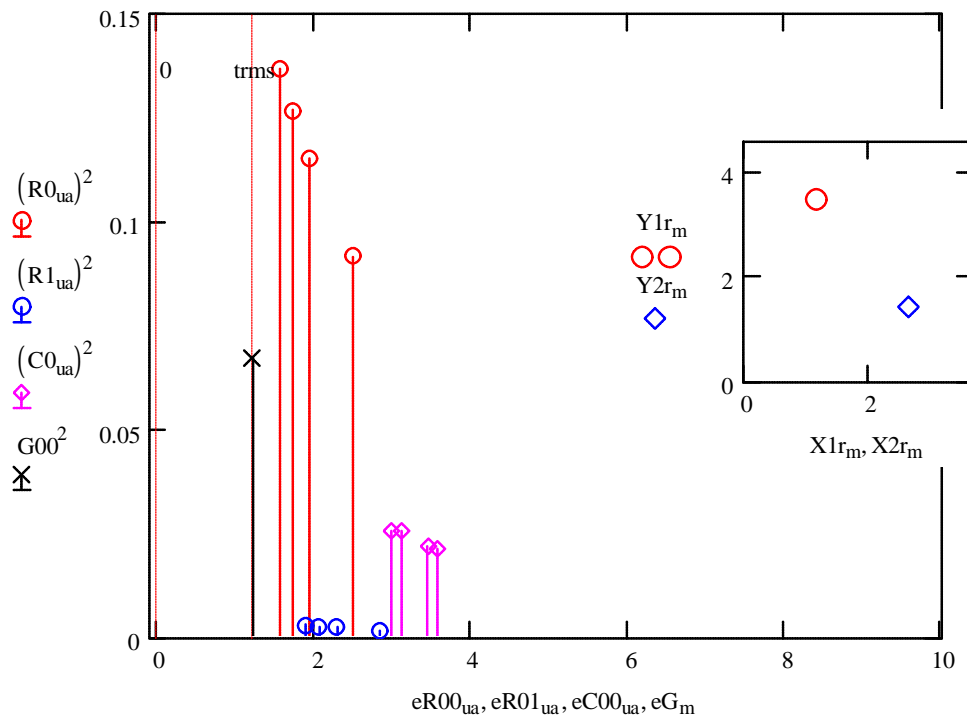


Figure 13. One particular realization of the LOS channel impulse energy response.

Plot the multiple realizations of the model:

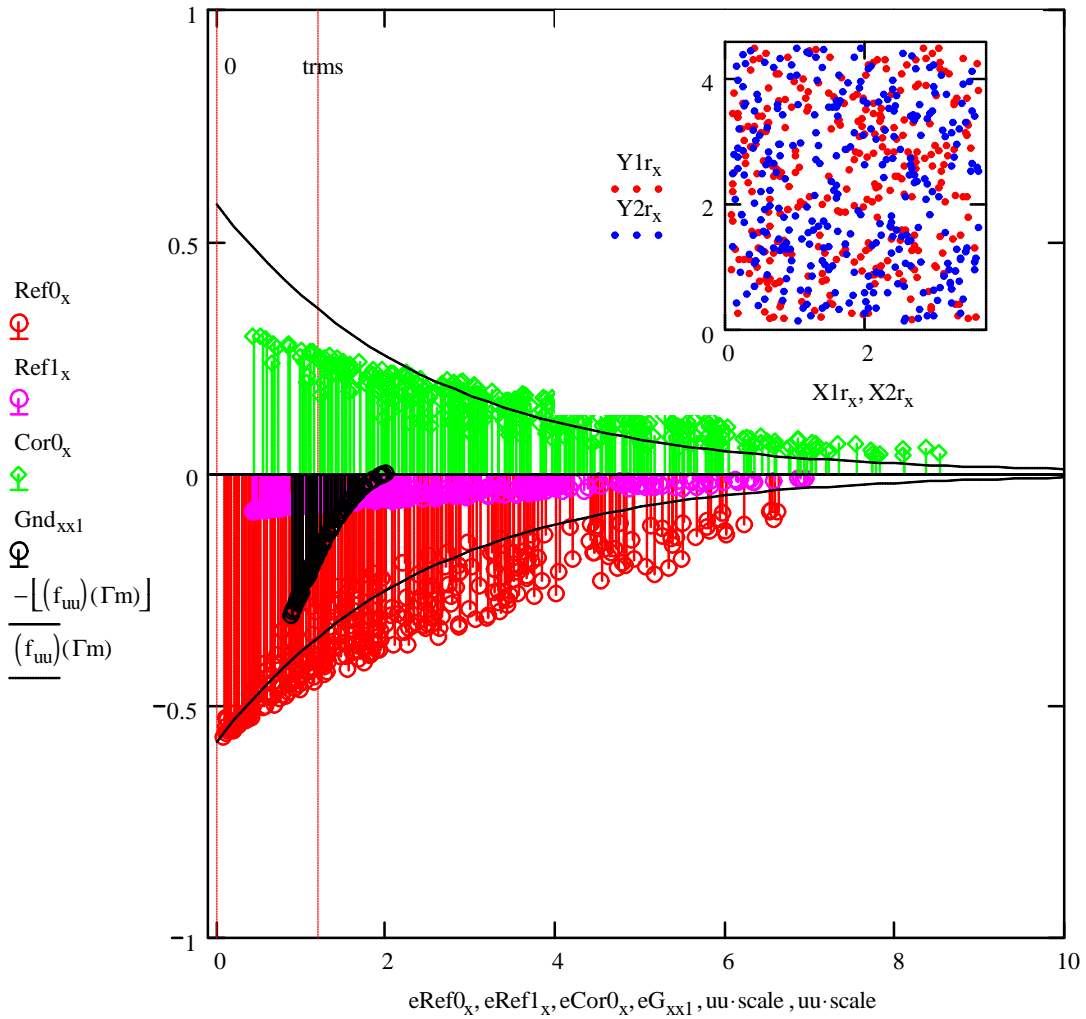


Figure 14. Multiple realizations of the LOS channel impulse amplitude responses.

The received energy by a "constant directivity" antenna aperture is:

$$W_{rx} := \frac{1.5}{4\pi} \cdot \frac{1}{f_2 - f_1} \cdot \left[\int_{f_1}^{f_2} \left(\frac{c}{f} \right)^2 \cdot \eta_{ant}(f) \cdot EIRP_{sd}(f) df \right]^2 \quad (25)$$

where:

$\eta_{ant}(f)$ is the antenna efficiency as a function of frequency

$EIRP_{sd}(f)$ is the radiated effective isotropically radiated power spectral density

Thus the collected signal at the receiver is:

$$S(t) := H_{LOSi}(t) \cdot \sqrt{W_{rx}} \quad (26)$$

Signal $S(t)$ contains all of the multipath components, weighted by the receiver antenna aperture, and by the receiver antenna efficiency. The method of signal detection, signal convolution the receiver filter, multiplication by the receiver template, and the signal processing will determine which and how many and how efficiently the multipath components are utilized.

The following parameters specific the UWB radio performance in a room-LOS condition:

- (1) Room dimensions RoomX and RoomY, and minimum distance to a wall d_t
- (2) Antenna heights h_1 and h_2
- (2) Radiated power spectral density $EIRP_{sd}(f)$
- (3) Receiver antenna aperture A_e
- (4) Multipath signal profile $S(t)$
- (5) Average reflection coefficient Γ_m

Derived parameters include:

- RMS delay spread τ_{rms} ,
- the mean ray arrival rate T_s
- excess energy factor in the room is W_x

Here: RoomX = 3.7 m and $\tau_{rms} = 4.008 \times 10^{-9}$ sec
 RoomY = 4.6 m $T_s = 7.423 \times 10^{-9}$ sec
 $h_1 = 1$ m
 $h_2 = 2$ m $W_x = 1.618$

Accounting for the total energy, the "excess" energy in the room W_x should approximately be balanced by the average wall-transmitted energy, thus: $10\log[(W_x)(1 + \Gamma_m^2)]$ should approximately equal 0 dB.

$$10 \cdot \log \left[(1 - \Gamma_m^2) \cdot W_x \right] = 0.31 \quad \text{dB} \quad (27)$$

Case 2: Non-Line of Sight Multipath Model

The Jakes [Jakes 1974] model with exponential EDP will be applied, here for UWB pulses in non-line of sight (NLOS) cases. Thus the multipath impulses are exponentially distributed, their arrival interval is randomly distributed in windows of duration T_s .

Jakes Channel Model for $f < 1000$ MHz follows.

To test the equations, let the initial delay spread equal τ_{rms} where $\tau_{rms} := 20 \cdot \text{nanosec}$

The mean ray T_m arrival interval is based on the LOS room model. A total of 13 paths with a mean delay of T_s were found. Thus the mean ray arrival interval is $2T_s/13$:

$$T_m := T_s \cdot \frac{2}{9} \quad T_m = 1.65 \times 10^{-9} \quad (28)$$

For now, we let T_{s1} be artificially small by a factor of R , as a calculation convenience to equivalently realize R of the channel model

$$R := 10$$

The maximum number of components considers is

$$K_{max} := \text{ceil}\left(10 \cdot \frac{\tau_{rms}}{T_m} \cdot R\right) \quad K_{max} = 1.213 \times 10^3 \quad k := 0..K_{max}$$

The multipath components are randomly distributed in "bins" that are T_s wide and spaced T_s .

$$T_k := \frac{T_m}{R} \cdot (k + \text{rnd}(1)) \quad T_0 = 9.686 \times 10^{-11} \quad (29)$$

Channel coefficient h is normally distributed with unity standard deviation:

$$h_k := \text{norm}(K_{max} + 1, 0, 1) \quad (30)$$

(sanity check): $\text{mean}(h_k) = -0.038$ $\text{stdev}(h_k) = 0.981$

$$\sigma_a := 1 - \exp\left(\frac{-T_m}{\tau_{rms} \cdot R}\right) \quad \sigma_a = 8.214 \times 10^{-3} \quad (31)$$

$$\sigma_k := \sqrt{\sigma_a} \cdot \exp\left(\frac{T_k}{\tau_{rms} \cdot 2}\right) \quad \sigma_0 = 0.09 \quad (32)$$

Check the result

$$\sigma_{2k} := (\sigma_k)^2 \quad \text{mean}(\sigma_{2k}) \cdot K_{max} = 0.995 \quad (33)$$

$$h_k^2 := \sigma_k \cdot h_k \quad h_{2k}^2 := (h_k)^2 \quad \text{mean}(h_{2k}^2) \cdot K_{max} = 0.991 \quad (34)$$

$$H_{\text{delay}} := \sqrt{\frac{\sigma_a}{e}} \quad H_{\text{delay}} = 0.055 \quad \tau_{\text{rms}} := 20 \cdot \text{nanosec} \quad \tau := \frac{\tau_{\text{rms}}}{\text{nanosec}}$$

$$t_u := 0..200 \quad z := \frac{-\tau_{\text{rms}}}{\text{nanosec}} \cdot 0.5$$

Square root of power delay profile

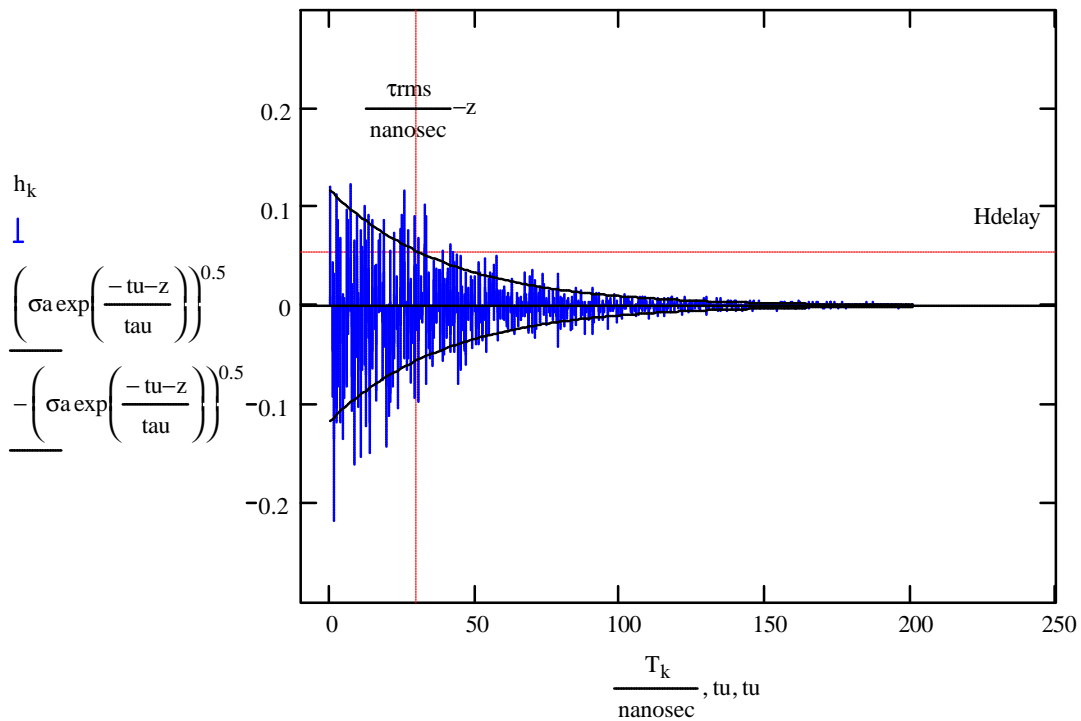


Figure 15. Multiple realizations of the NLOS channel model at a fixed distance.

NLOS multipath model: $K_{\text{max}} = 1.213 \times 10^3$

$$H_{\text{NLOS}}(t) := \text{Vfs}(d) \cdot \sqrt{Kf} \cdot \delta(0) + \left(\sqrt{1 - Kf} \cdot \sum_{k=0}^{K_{\text{max}}} h_k \cdot \delta(t - T_{s_k}) \cdot \left(\text{Vfs}(d + c \cdot T_{s_k}) \cdot \delta\left(t - \frac{T_{s_k}}{c}\right) \right) \right)^2 \quad (35)$$

The received signal is given by equation (25).

Thus the collected signal at the receiver is:

$$S_N(t) := H_{\text{NLOS}}(t) \cdot \sqrt{W_{\text{rx}}} \quad (36)$$

The delay spread parameter is a function of distance, [Siwiak 2003], and here is modeled by the square root of distance, see slide 34 of [IEEE802 04/504]. Thus

$$\tau_{\text{rmsN}}(d, D_t, \tau_0) := \tau_0 \sqrt{\frac{d}{D_t}} \quad (37)$$

A value for τ_0 and D_t that approximately match channel models CM2, CM3, and CM4 in their appropriate distances [IEEE802 02/249] is:

$$\tau_0 := 5.5 \quad D_t := 1 \quad (38)$$

Thus	$\tau_{\text{rmsN}}(2, D_t, \tau_0) = 7.778$	$\tau_{\text{rmsN}}(5, D_t, \tau_0) = 12.298$
	$\tau_{\text{rmsN}}(7, D_t, \tau_0) = 14.552$	$\tau_{\text{rmsN}}(10, D_t, \tau_0) = 17.393$
	$\tau_{\text{rmsN}}(20, D_t, \tau_0) = 24.597$	$\tau_{\text{rmsN}}(30, D_t, \tau_0) = 30.125$
	$\tau_{\text{rmsN}}(50, D_t, \tau_0) = 38.891$	
	$\tau_{\text{rmsN}}(100, D_t, \tau_0) = 55$	

The choice of trms increasing as the squareroot of distance will result in an average power law behavior of approximately 2.5 for a receiver not employing a rake or channel equalization technique.

Signal SN(t) contains all of the multipath components, weighted by the receiver antenna aperture, and by the receiver antenna efficiency. The method of signal detection, signal convolution the receiver filter, multiplication by the receiver template, and the signal processing will determine which and how many and how efficiently the multipath components are utilized.

The following parameters specific the UWB radio performance in a N-LOS condition:

- (1) RMS delay spread parameter τ_0 s multiplied by the square root of d/D_t
- (2) Mean interval between rays T_m s
- (3) Fraction of energy in direct ray K_f
- (4) Radiated power spectral density EIRPsd(f)
- (5) Receiver antenna aperture A_e
- (6) Multipath signal profile SN(t)

The Ricean K factor and K_f are related by: $K_f = K/(K+1)$, or equivalently $K = K_f/(1-K_f)$, where K_f takes on the range [0, 1] where correspondingly, K takes on the range [0, ∞].

Here: $\tau_0 = 5.5$ nanosec

$$\frac{T_m}{\text{nanosec}} = 1.65 \quad \text{nanosec}$$